The Sterol Carrier Protein-2 Amino Terminus: A Membrane Interaction Domain†

Huan Huang,‡ Judith M. Ball,§ Jeffrey T. Billheimer,|| and Friedhelm Schroeder*,‡

Department of Physiology and Pharmacology and Department of Pathobiology, Texas A&M University, TVMC, College Station, Texas 77843-4466, and Cardiovascular Department, DuPont Merck Pharmaceutical Company, Experimental Station 400-3231, Wilmington, Delaware 19898-0400

Received April 15, 1999; Revised Manuscript Received July 21, 1999

ABSTRACT: Sterol carrier protein-2 (SCP_2) is a small, 123 amino acid, protein postulated to play a role in intracellular transport and metabolism of lipids such as cholesterol, phospholipids, and branched chain fatty acids. While it is thought that interaction of SCP_2 with membranes is necessary for lipid transfer, evidence for this possibility and identification of a membrane interaction domain within SCP_2 has remained elusive. As shown herein with circular dichroism and a direct binding assay, SCP_2 bound to small unilamellar vesicle (SUV) membranes to undergo significant alteration in secondary structure. The SCP_2 amphipathic N-terminal 32 amino acids, comprised of two α-helical segments, were postulated to represent a putative phospholipid interaction site. This hypothesis was tested with a series of SCP_2 N-terminal peptides, circular dichroism, and direct binding studies. The SCP_2 N-terminal peptide $^{1-32}SCP_2$, primarily random coil in aqueous buffer, adopted α-helical structure upon interaction with membranes. The induction of α-helical structure in the peptide was maximal when the membranes contained a high mole percent of negatively charged phospholipid and of cholesterol. While deletion of the second α-helical segment within this peptide had no effect on formation of the first α-helix, it significantly weakened the peptide interaction with membranes. Substitution of Leu^{20} with Glu^{20} in the N-terminal peptide disrupted the α-helix structure and greatly weakened the peptide interaction with membranes. Finally, deletion of the first nine nonhelical amino acids had no effect either on formation of α-helix or on peptide binding to membranes. N-Terminal peptide $^{1-32}SCP_2$ competed with SCP_2 for binding to SUV. These data were consistent with the N-terminus of SCP_2 providing a membrane interaction domain that preferentially bound to membranes rich in anionic phospholipid and cholesterol.

The physiological function of sterol carrier protein-2 (SCP_2)[1] is not known. In vitro data suggest that SCP_2 participates in intracellular transport and metabolism of lipids such as cholesterol (reviewed in refs *1*−*8*), glycerides,[2] fatty acids (*9*−*11*),[3] isoprenoids (*12*, *13*), and branched chain fatty acids (*12*, *14*, *15*). The expression of SCP_2 is associated with lung surfactant formation (*16*), diabetes (*17*), sterol oxidation (*18*−*20*), and biliary cholesterol transport (*19*, *21*−*24*). Overexpression of SCP_2 in transfected cells increased mitochondrial cholesterol oxidation (*25*), while introduction of anti-SCP_2 antibodies inhibited mitochondrial corticosteroid formation (*26*, *27*). Overexpression of SCP_2 in transfected cells also enhanced cholesterol uptake (*28*, *29*), transfer of plasma membrane derived cholesterol to the endoplasmic reticulum (*30*), transfer of cholesterol from the endoplasmic reticulum to the plasma membrane (*31*), and intracellular cholesterol esterification and triacylglycerol formation (*29*, *30*). Gene ablation of SCP_2 in mice resulted in decreased liver cholesterol ester and triglyceride content as well as impaired ability to oxidize branched chain fatty acids (*15*). In summary, the available evidence obtained in vitro, in vivo, and in intact cells suggests that SCP_2 is involved in transport, metabolism, and/or secretion of cholesterol as well as other lipids.

Although the mechanism whereby SCP_2 elicits the above activities is not entirely clear, recent studies with model (reviewed in refs *3*−*5* and *32*) and biological membranes

† This work was supported in part by grants from the National Institutes of Health (GM31651 and DK41402).

* To whom correspondence should be addressed. Tel: 409-862-1433. Fax: 409-862-4929. E-mail: fschroeder@cvm.tamu.edu.

‡ Department of Physiology and Pharmacology, Texas A&M University.

§ Department of Pathobiology, Texas A&M University.

|| DuPont Merck Pharmaceutical Co.

[1] Abbreviations: SCP_2, sterol carrier protein-2; $^{1-24}SCP_2$, Ser-Ser-Ala-Ser-Asp-Gly-Phe-Lys-Ala-Asn-Leu-Val-Phe-Lys-Glu-Ile-Glu-Lys-Lys-Leu-Glu-Glu-Glu-Gly-NH_2; $^{1-32}SCP_2$, Ser-Ser-Ala-Ser-Asp-Gly-Phe-Lys-Ala-Asn-Leu-Val-Phe-Lys-Glu-Ile-Glu-Lys-Lys-Leu-Glu-Glu-Glu-Gly-Glu-Gln-Phe-Val-Lys-Lys-Ile-Gly-NH_2; $^{10-32}SCP_2$, Asn-Leu-Val-Phe-Lys-Glu-Ile-Glu-Lys-Lys-Leu-Glu-Glu-Glu-Gly-Glu-Gln-Phe-Val-Lys-Lys-Ile-Gly-NH_2; $^{1-E20-32}SCP_2$, $^{1-32}SCP_2$, Ser-Ser-Ala-Ser-Asp-Gly-Phe-Lys-Ala-Asn-Leu-Val-Phe-Lys-Glu-Ile-Glu-Lys-Lys-Glu-Glu-Glu-Glu-Gly-Glu-Gln-Phe-Val-Lys-Lys-Ile-Gly-NH_2; HOAT, 1-hydroxy-7-azabenzotriazole; Fmoc, fluorenylmethoxycarbonyl; TFA, trifluoroacetic acid; TFE, trifluoroethanol; HPLC, high-performance liquid chromatography; MALDI/TOF, matrix-assisted laser desorption ionization/time of flight; MOPS, 3-(*N*-morpholino)propanesulfonic acid; SUV, small unilamellar vesicles; POPC, 1-palmitoyl-2-oleoyl-*sn*-glycero-3-phosphocholine; DOPS, 1,2-dioleoyl-*sn*-glycero-3-phospho-L-serine.

[2] O. Starodub, B. P. Atshaves, J. B. Roths, J. Schoer, C. J. Jolly, A. B. Kier, and F. Schroeder, Sterol carrier protein-2 expression and intracellular localization in transfected L-cell fibroblasts, submitted for publication, 1999.

[3] N. J. Stolowich, A. Frolov, A. D. Petrescu, A. L. Scott, J. T. Billheimer, and F. Schroeder, Holo-Sterol Carrier Protein-2: ^{13}C NMR Investigation of Cholesterol and Fatty Acid Binding Sites, revision pending for publication, 1999.

10.1021/bi990870x CCC: $18.00
Published on Web 09/16/1999

(reviewed in refs *1*, *3*−*5*, *18*, *33*, and *34*) have yielded the following important insights: (i) With few exceptions (*35*), most reports support that SCP_2 binds cholesterol (*2*, *36*−*40*).[3] (ii) The SCP_2 cholesterol binding site appears essential for SCP_2-mediated intermembrane sterol transfer (*41*). (iii) SCP_2-mediated intermembrane sterol transfer is vectorial (*42*, *43*). (iv) Removal of the SCP_2 10 amino-terminal residues or replacing Leu^{20} with Glu^{20} altered the circular dichroic spectrum of SCP_2 to dramatically reduce α-helix content and completely abolish SCP_2-mediated intermembrane sterol transfer activity (*44*). However, it is not known whether this was due to disruption of the cholesterol binding site or of a putative membrane interaction site. (v) Because SCP_2-enhanced intermembrane sterol transfer was greatest (several orders of magnitude higher) in membranes containing anionic phospholipids, it is thought that ionic interactions of the basic SCP_2 with the acidic phospholipids may mediate binding of the protein to the membrane (*32*, *45*−*49*). These data are consistent with the hypothesis that membrane interaction may be required for SCP_2-mediated cholesterol transfer.

Over a decade ago it was postulated that the SCP_2 N-terminus may form an amphipathic α-helix stabilized by interaction with membranes, i.e., represents a putative membrane interaction site (*50*). However, proof for this hypothesis has been lacking. Furthermore, it is not known whether the putative membrane interaction domain of SCP_2 may also be responsible for eliciting intermembrane lipid transfer. Because the functional domains of SCP_2 protein have not been characterized, the purpose of the present investigation was to structurally and functionally characterize the SCP_2 N-terminal region comprising a putative membrane interaction site. Several questions were addressed: (i) Do SCP_2 and its N-terminal peptides interact with lipid membranes? (ii) Are there secondary structural changes in the protein and/or peptides upon such interaction? (iii) What are the structural requirements of the SCP_2 N-terminal peptides necessary for membrane interaction? (iv) What are the membrane lipid compositional requirements needed for interaction of SCP_2 and N-terminal peptides with membranes? These issues were resolved using circular dichroism, membrane binding assays, and synthetic N-terminal peptides.

EXPERIMENTAL PROCEDURES

Materials. 1-Palmitoyl-2-oleoyl-*sn*-glycero-3-phosphocholine (POPC) and 1,2-dioleoyl-*sn*-glycero-3-phospho-L-serine (DOPS) were purchased from Avanti Polar Lipids (Alabaster, AL). Cholesterol, *o*-phthaldialdehyde, trifluoroethanol (TFE), and *β*-mercaptoethanol were acquired from Sigma (St. Louis, MO). Microcon-100 filtration units were purchased from Fisher Scientific Inc. (Pittsburgh, PA). Recombinant human liver SCP_2 was prepared as described previously (*51*).

Peptide Synthesis. Peptides were synthesized by fluorenylmethoxycarbonyl (Fmoc) solid-phase chemistry employing a Millipore 9050 Plus (Perceptive Biosystems, Framingham, MA) automated peptide synthesizer (Peptide Synthesis Core Facility, Texas A&M University, directed by Dr. Judith Ball). The automated synthesizer was computer driven with algorithms that were easily adjusted and accommodated alterations in reaction times, activation chemistry, and reagent volumes. The activation chemistry employed was 1-hydroxy-7-azabenzotriazole (HOAT) with diisopropylcarbodiimide. One gram of the poly(ethylene glycol) resin with PAL linker yielded between 300 and 500 mg of pure peptide product. Cleavage of the final peptide product from the solid polymer support and removal of side chain protecting groups were facilitated by the addition of 90% trifluoroacetic acid (TFA) in the presence of ethanedithiol (3%), thioanisole (5%), and anisole (2%). Following a 2 h incubation, the cleavage mixture containing the cleaved peptide was filtered into a polypropylene tube containing cold diethyl ether, and the resin was rinsed several times with TFA to ensure the complete recovery of the cleaved peptide. The peptide was then extracted with cold diethyl ether an additional two times and dried under compressed nitrogen gas prior to lyophilization.

Peptide Purification and Characterization. As a peptide sequence increases in length, the opportunity for synthetic errors, undesirable modifications, and cumulative effects arising from incomplete reactions grows (*52*). Consequently, the correctness and purity of the covalent structure and the presence of unwanted peptide byproducts were determined. Crude peptide was subjected to large-scale, gravimetric gel filtration chromatography to remove organic contaminants and to partially separate incomplete peptides on the basis of molecular weight. Peptide components were detected at 215 nm using a model 229 UV/vis detector (ISCO, Lincoln, NB). Fractions that correspond to absorbance peaks were collected and lyophilized. The second purification step was reverse-phase HPLC using a C4 column (Waters, Milford, MA). Eluted peptides were detected at 220 nm.

Matrix-assisted laser desorption ionization/time of flight (MALDI/TOF) provides a direct means of discerning the full-length peptide product and any byproduct that differs from the target peptide theoretical molecular weight. PDMS was performed on each peptide (Laboratory for Biological Mass Spectrometry, Department of Chemistry, Texas A&M University, College Station, TX). Those peptides with a correct theoretical mass corresponding to 90% or greater of the final peptide product were used in our experimental assays. Those peptides that did not contain the correct theoretical mass were resynthesized and reevaluated prior to use.

Peptide Amino Acid Analysis. Peptide concentration of the stock solution was determined by peptide amino acid analysis which was performed at the Protein Chemistry Laboratory, Department of Chemistry, Texas A&M University. Amino acid analysis was determined using a AminoQuant II System (Hewlett-Packard Inc., Palo Alto, CA) consisting of an HP 1090 liquid chromatograph with an Hewlett-Packard Chemstation. Peptides were analyzed by precolumn derivatization of hydrolyzed samples with *o*-phthalaldehyde and 9-(fluoromethyl)chloroformate (Fmoc). *o*-Phthalaldehyde reacts rapidly with primary amino acids and Fmoc rapidly with secondary amino acids (proline) quantitatively to yield highly fluorescent and UV-absorbing isoindole derivatives. The latter were separated by reverse-phase HPLC and detected by UV absorbance with a diode array detector or by fluorescence with an in-line fluorescence detector. Samples were mixed with internal standard, dried in vacuo, and vapor phase hydrolyzed with 6 N HCl at 110 °C for 24 h under Ar in the presence of phenol. The samples were reconstituted in borate buffer for AminoQuant analysis.

Membrane Vesicle Preparation. Small unilamellar vesicles (SUV) were designated as neutral zwitterionic when com-

posed of POPC/cholesterol (molar ratio 65:35) or negatively charged (anionic) when composed of POPC/cholesterol/DOPS (molar ratios 90:0:10, 70:20:10, 55:35:10, and 40:50:10, respectively). SUV were prepared as described earlier (*32*, *53*) with some modifications. Lipids from $CHCl_3$ stocks were mixed in a small amber vial and dried under a stream of N_2. With constant rotation of the vial, the dry lipids formed a thin film on the wall and dried under vacuum for at least 4 h or overnight to remove any residual organic solvent present. The lipids were hydrated by vortexing in MOPS buffer (10 mM, pH = 7.4, prefiltered through a 0.2 μM filter) (Millipore, Bedford, MA). The resulting suspension was sonicated under N_2 protection in a cold water bath, using a microprobe with a Sonic Dismembrator, Model 550 (Fisher Scientific Inc., Pittsburgh, PA). The energy was set at level 4 with 1 min pause after every 2 min sonication to prevent overheating of the lipid solution. The sonicated solution was certrifuged using a 40Ti rotor (Beckman Instruments, Fullerton, CA) at 35 K for 4 h to remove any multilamellar vesicles and any titanium debris from the sonicator probe. The lipid concentration of the final SUV solution was determined by phosphate assay (*54*).

Circular Dichroism. Circular dichroism was performed basically as described earlier (*10*). Briefly, the samples contained peptide (15 μM) or protein (4 μM) with or without SUV (1 mM). Background samples were composed of buffer or lipid vesicles without peptide or protein. Circular dichroic measurements were taken on a JASCO J-710 spectropolarimeter (JASCO Inc., Easton, MD) using a 1 mm circular quartz cell at room temperature. The spectra were taken from 185 to 260 nm with 1 nm step resolution, speed 50 nm/min, response 1 s, bandwidth 2.0 nm, and sensitivity 10 mdeg. For each measurement, five to ten scans were averaged, smoothed, background subtracted, and converted to mean residue molar ellipticity [θ] (deg cm^2 dmol^{-1}). The percent α-helix for the peptides was calculated according to the equation:

$$\theta_{222} = (f_h - i\kappa/N)[\theta_{h\ 222\infty}] \quad (1)$$

where θ_{222} is the mean residue molar ellipticity at 222 nm, $\times a6_h$ is the fraction in α-helical form, i is the number of helices, κ is a wavelength-specific constant with a value of 2.6 at 222 nm, N is the number of residues in the peptide, $\theta_{h\ 222\infty}$ is the molar ellipticity for a helix of infinite length at 222 nm and has a value of −39 500 deg cm^2 dmol^{-1} (*55*, *56*). The percent α-helix for the protein was also calculated by the program SELCON provided by JASCO. In this program, the spectrum of the protein to be analyzed was included in the basis set, and an initial estimation was made for the unknown structure as a first approximation. The resulting matrix equation was solved using the singular value decomposition algorithm, and the initial estimate was replaced by the solution to the equation. This process was repeated until self-consistency was attained (*57*). Both methods were in good agreement in providing the percent α-helix.

Transbilayer Distribution of Phosphatidylserine. The transbilayer distribution of phosphatidylserine in SUV was determined as described previously (*58*).

SCP_2-Vesicle Binding Assay. The binding of SCP_2 to SUV (POPC:cholesterol:DOPS = 35:35:30) was determined by incubating SCP_2 (1.55 nmol) with SUV (0−200 nmol) in a total volume of 200 μL at room temperature for 10 min. The solutions were transferred to Microcon-100 filtration units (molecular weight cutoff 100 000) and centrifuged at 3000*g* for 5 min. The filter was rinsed by adding a 100 μL aliquot of buffer solution and centrifuging at 3000*g* for another 3 min. The flow-through fractions, which contained free (unbound) SCP_2, were saved for analysis. The membrane filter bound SCP_2 was recovered by placing the filtration unit upside down in a new vial and centrifuging for 30 s as above. A 100 μL solution of buffer, 0.1 M NaCl, and 0.15 mM Triton X-100 was then added, and the upside down filter unit was centrifuged as above for 30 s after each addition. The free and membrane-bound SCP_2 fractions were then analyzed by SDS−PAGE. Quantitation was performed by comparison to a standard curve comprised of a series of standard solutions of known SCP_2 concentration run on the same gel in adjacent lanes. After staining and destaining, gel images were acquired with a model IS-500 system composed of a single-chip charge couple device video camera and computer workstation (Alpha Innotech, San Leandro, CA). The images were analyzed (mean 8-bit gray scale) using NIH Image (written by W. Rasband and available by anonymous FTP from zippy.nimh.nih.gov) on a Power Macintosh workstation.

Peptide−Vesicle Binding Assay. The peptide−vesicle binding assay was performed as described earlier (*59*, *60*). Peptide (12 nmol) and SUV (800 nmol) were incubated at room temperature for 10 min in a total volume of 200 μL of 10 mM MOPS buffer (pH = 7.4). Samples containing only the peptide and only the SUV were used as controls and blanks. Samples were then transferred to a Microcon-100 filtration unit (molecular weight cutoff of 100 000) and centrifuged at 3000g for 5−10 min, until all but 5−10 μL had gone through the filter. The filter was rinsed with 100 μL of buffer and centrifuged again for 3−5 min. Unbound peptide in the flow-through fraction was quantified with an *o*-phthaldialdehyde assay (below).

To 100 μL of the flow-through peptide solution was added 0.5 mL of 0.05 M sodium borate (pH 10) and 0.5 mL of 0.5% (v/v) β-mercaptoethanol in ethanol, vortexing well after each addition. *o*-Phthaldialdehyde (10 mg/mL) in methanol was diluted 10-fold in 0.05 M borate (pH 10), and 0.5 mL of this solution was added to the peptide assay solution and vortexed well. The samples were incubated at room temperature for exactly 20 min before measurement on a PC1 Photon Counting fluorescence spectrophotometer (ISS Inc., Champaign, IL). The fluorescence intensity (excitation at 340 nm, emission at 440 nm) was measured for each sample. The standard curve for *o*-phthaldialdehyde assay of each peptide was obtained by measurement of a 100 μL peptide solution contained 0−6 nmol of the peptides.

Displacement of SUV-Bound SCP_2 by Peptide. SCP_2 (1.55 nmol) was added to 60 nmol of SUV (POPC:cholesterol:DOPS = 35:35:30) and incubated with $^{1-32}SCP_2$ (from 0 to 39 nmol) in a total volume of 200 μL at room temperature for 10 min. The free (unbound) and bound SCP_2 were separated using the Microcon-100 molecular weight cutoff centrifuge filter and quantitated by SDS gel as described for above for the SCP_2−SUV binding assay.

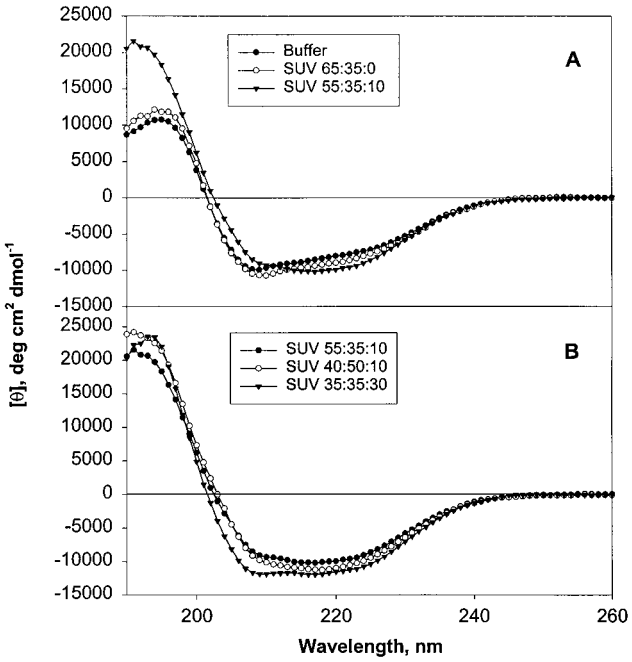

FIGURE 1: Effect of SUV lipid composition on circular dichroic spectra of SCP_2 protein. Circular dichroic spectra were obtained as described in Experimental Procedures. Panel A: Symbols represent SCP_2 CD spectra taken in the presence of (●) buffer only; (○) SUV, POPC:cholesterol:DOPS = 65:35:0; and (▼) SUV, POPC:cholesterol:DOPS = 55:35:10. Panel B: Symbols represent the CD spectra of SCP-2 taken in the presence of (●) SUV, POPC:cholesterol:DOPS = 55:35:10; (○) SUV, POPC:cholesterol:DOPS = 40:50:10; and (▼) SUV, POPC:cholesterol:DOPS = 35:35:30.

Table 1: Effect of SUV Lipid Composition on α-Helical Content of SCP_2

SUV lipid composition[a]	% α-helix[b]
buffer	29.2 ± 0.9
SUV, 65:35:0	31.0 ± 0.6
SUV, 55:35:10	34.2 ± 1.6
SUV, 40:50:10	35.8 ± 1.0
SUV, 35:35:30	36.6 ± 1.2

[a] Lipid compositions are presented as the molar ratio of POPC:cholesterol:DOPS. [b] α-Helical contents were presented as the mean ± SD ($n = 4$), calculated on the basis of circular dichroic spectra obtained from SCP_2 (4 μM) in the presence of buffer or SUV (1 mM).

RESULTS

Interaction of SCP_2 with SUV. Circular dichroism measurements were conducted to monitor the changes in SCP_2 secondary structure upon interaction with lipid vesicles. Small unilamellar vesicles (SUV) containing varying amounts of POPC (neutral lipid), cholesterol (sterol), and DOPS (anionic lipid) were used as model membranes to study the effect of lipid composition on the interaction of SCP_2 with membranes.

SCP_2 in aqueous buffer displayed circular dichroic spectra consistent with significant α-helix content: negative ellipticity of −8200 deg cm^2 dmol^{-1} at 222 nm; large positive ellipticity of +23 500 deg cm^2 dmol^{-1} at 190 nm (Figure 1A, solid circles). The percentage of α-helix was estimated to be 29% (Table 1) using the SELCON program as described in Experimental Procedures.

In the presence of neutral SUV-containing POPC/cholesterol at a molar ratio of 65:35, the circular dichroic spectrum of SCP_2 changed only slightly compared to SCP_2 alone in aqueous buffer (Figure 1A, open vs solid circles). It was estimated using the program SELCON that the percent α-helix increased only from 29% to 31% (Table 1). However, this change was not statistically significant.

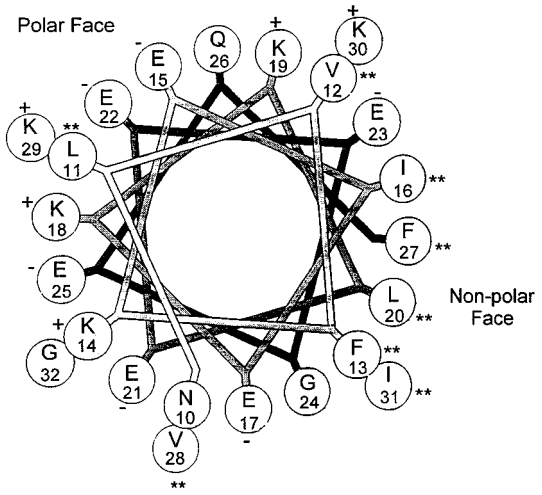

FIGURE 2: Helical wheel diagrams of the SCP_2 N-terminal α-helical region (amino acids 10−32). Symbols represent (+) positively charged amino acids, (−) negatively charged amino acids, and (**) hydrophobic amino acids.

In the presence of anionic SUV containing POPC/cholesterol/DOPS (molar ratio 55:35:10) larger circular dichroic spectral changes were observed in SCP_2. The molar ellipticity at 222 nm became more negative as compared to SCP_2 in buffer alone (−11 200 vs −8200 deg cm^2 dmol^{-1}). Concomitantly, the SCP_2 molar ellipticity at 190 nm increased 2.2-fold as compared to SCP_2 in buffer alone (23 500 vs 10 500 deg cm^2 dmol^{-1}). Calculations showed that the α-helix content of SCP_2 increased significantly ($p < 0.001$, $n = 4$) from 29.2 ± 0.9% to 34.2 ± 1.6% in the presence of anionic SUV (Table 1). In the presence of increasing anionic phospholipid content in the SUV, the circular dichroic spectra of SCP_2 shifted even more in favor of α-helical structure such that at 30 mol % anionic phospholipid the quantity of SCP_2 α-helix was 36.6 ± 1.2% (Figure 1B and Table 1).

In summary, the circular dichroism data showed that SCP_2 protein preferentially interacted with SUV-containing anionic phospholipid and that SCP_2 underwent secondary structural changes favoring as much as an 8% increase in α-helix formation upon SCP_2 interation with anionic membranes. This finding was distinct from that observed for interaction of SCP_2 with cholesterol in buffer alone (i.e., in the absence of membranes) where a 3% decrease in α-helix content of SCP_2 was reported (*37*).

SCP_2 N-Terminal Peptides. Several SCP_2 N-terminal peptides were designed and assayed to determine some of the structural features of the N-terminus necessary for interaction with membranes. The peptides selected were based on the solution structure of SCP_2 determined by NMR (*61*) and on site-directed mutagenesis of SCP_2 (*44*). Previous NMR studies showed that the SCP_2 N-terminus is comprised of two α-helical regions, peptide residues 9−22 and 25−30. Figure 2 shows the helical wheel projection of the N-terminal α-helical region (amino acids 10−32). It shows amphipathic character of this region with a highly charged polar face, rich in positively charged amino acids, and a nonpolar face.

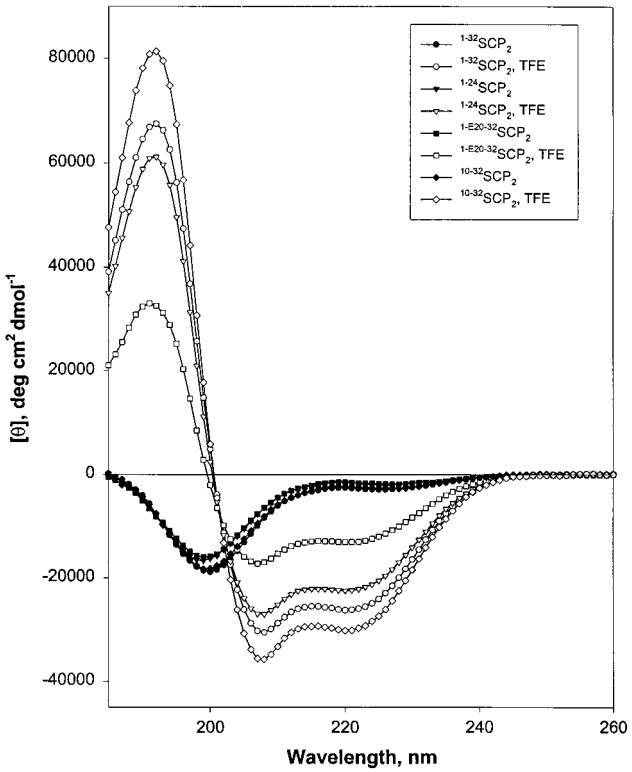

FIGURE 3: Circular dichroic spectra of SCP_2 N-terminal peptides in aqueous buffer and 50% TFE. Circular dichroic spectra were obtained as described in Experimental Procedures. Symbols represent (●) peptide $^{1-32}SCP_2$ in buffer; (▼) peptide $^{1-24}SCP_2$ in buffer; (■) peptide $^{1-E20-32}SCP_2$ in buffer; (◆) peptide $^{10-32}SCP_2$ in buffer; (○) peptide $^{1-32}SCP_2$ in TFE/water (1:1); (▽) peptide $^{1-24}SCP_2$ in TFE/water (1:1); (□) peptide $^{1-E20-32}SCP_2$ in TFE/water (1:1); and (◇) peptide $^{10-32}SCP_2$ in TFE/water (1:1).

Four peptides were synthesized and examined. First, peptide $^{1-32}SCP_2$, corresponding to residues 1−32 of the SCP_2 N-terminus, contained both of the predicted α-helical regions. Peptide $^{1-32}SCP_2$ had a net charge of −1 (seven negatively charged vs six positively charged residues).

Second, peptide $^{1-24}SCP_2$, corresponding to residues 1−24 of the SCP_2 N-terminus, contained only the first predicted helix. Peptide $^{1-24}SCP_2$ had a net charge of −2 (six negatively charged vs four positively charged residues).

Third, peptide $^{1-E20-32}SCP_2$ corresponds to the same sequence as $^{1-32}SCP_2$ except Leu^{20} was substituted with Glu^{20}. This substitution in the intact SCP_2 protein inactivated the protein in sterol exchange (*44*). Peptide $^{1-E20-32}SCP_2$ had a net charge of −2 (eight negatively charged vs six positively charged residues).

Fourth, $^{10-32}SCP_2$, corresponding to residues 10−32 of the SCP_2 N-terminus, contained both of the predicted helical regions with deletion of the nonhelical N-terminal nine amino acids. This deletion in the intact SCP_2 protein inactivated the protein in sterol exchange (*44*). Peptide $^{10-32}SCP_2$ had a net charge of −1 (six negatively charged vs five positively charged residues).

Secondary Structure of SCP_2 Amino-Terminal Peptides in Aqueous Buffer. The secondary structure of SCP_2 N-terminal peptides $^{1-32}SCP_2$, $^{1-24}SCP_2$, $^{1-E20-32}SCP_2$, and $^{10-32}SCP_2$ in aqueous buffer was determined by circular dichroism. Circular dichroic spectra of all four peptides (Figure 3, filled symbols) showed a large minimum at 200 nm and a small minimum at 222 nm indicative of predominantly random structure with only a small amount of α-helix. The estimated percent α-helix was 15% for $^{1-32}SCP_2$ and $^{1-24}SCP_2$, 12% for $^{1-E20-32}SCP_2$, and 18% for $^{10-32}SCP_2$ (Table 2).

Table 2: Effect of Solvent and Membrane on α-Helix Formation by SCP_2 N-Terminal Peptides

	% α-helix[a]		
peptides	buffer	50% TFE[b]	SUV (35:35:30)[c]
$^{1-32}SCP_2$	15.0 ± 0.1	75.3 ± 1.9	60.3 ± 0.2
$^{1-24}SCP_2$	15.0 ± 0.2	66.7 ± 0.5	36.9 ± 0.3
$^{1-E20-32}SCP_2$	12.2 ± 0.1	40.8 ± 0.3	20.6 ± 0.2
$^{10-32}SCP_2$	17.9 ± 0.3	86.2 ± 0.6	72.9 ± 1.8

[a] The α-helical contents are described as the mean ± SD (n=4). [b] TFE:aqueous buffer = 1:1. [c] POPC:cholesterol:DOPS.

Since aqueous buffers do not favor spontaneous formation of α-helix by peptides, a different solvent system was used to test whether these peptides had similar α-helix-forming potential. Trifluoroethanol (TFE) favors secondary structure in peptides and proteins by promoting intramolecular hydrogen bonding (*62*). Therefore, the propensity for the peptides to form helical structures can be determined by measuring circular dichroic spectra in aqueous solution containing TFE. The circular dichroic spectra of each peptide in TFE/water (1:1) differed markedly from those in aqueous buffer. The circular dichroic spectrum of each peptide in TFE/water (1:1) indicated the presence of a large proportion of α-helical structure, with the characteristic negative minimum at 208 and 222 nm and a positive maximum at 190 nm (Figure 3, open symbols). The α-helical content for peptide $^{1-32}SCP_2$ in TFE/water (1:1) was 75% (Table 2), suggesting that about 24 amino acids adopted the α-helical conformation, while 8 amino acids were nonhelical. This was consistent with the NMR data of the SCP_2 protein (*61*) which suggested that the first 9 amino acids of the SCP_2 N-terminus are nonhelical. In TFE/water (1:1) peptide $^{1-24}SCP_2$ exhibited 67% α-helix (Table 2), consistent with 16 helical amino acids and 8 nonhelical amino acids. Thus, deletion of the second helical region of $^{1-32}SCP_2$ to form $^{1-24}SCP_2$ had no effect on the ability of the first predicted helix to form. Peptide $^{1-E20-32}SCP_2$ showed only 41% α-helix (Table 2), consistent with 13 helical amino acids and 19 nonhelical amino acids. Thus, compared with $^{1-32}SCP_2$, substitution of Leu^{20} with Glu^{20} substantially reduced the ability of the peptide to form α-helix structure. Finally, peptide $^{10-32}SCP_2$ showed 86% α-helix (Table 2), suggesting 20 helical amino acids and 3 nonhelical amino acids. This indicated that the first 9 nonhelical amino acids were not necessary for the rest of the peptide to form α-helix structure.

Effects of Anionic Phospholipids on Membrane Interaction of SCP_2 N-Terminal Peptides. Since the presence of increasing amounts of anionic phospholipid in the SUV membranes elicited larger circular dichroic changes upon SCP_2 interaction, the effect of SUV anionic phospholipid content on N-terminal peptide interaction was examined (Figure 4). The circular dichroic spectrum and calculated α-helix content of peptide $^{1-32}SCP_2$ were not significantly altered by the presence of neutral vesicles comprised of POPC:cholesterol [molar ratio 65:35 (Figure 4A and Figure 5A) or molar ratio 50:50 (data not shown)]. In contrast, in the presence of negatively charged SUV, i.e., SUV containing the anionic phospholipid phosphatidylserine (DOPS), the circular di-

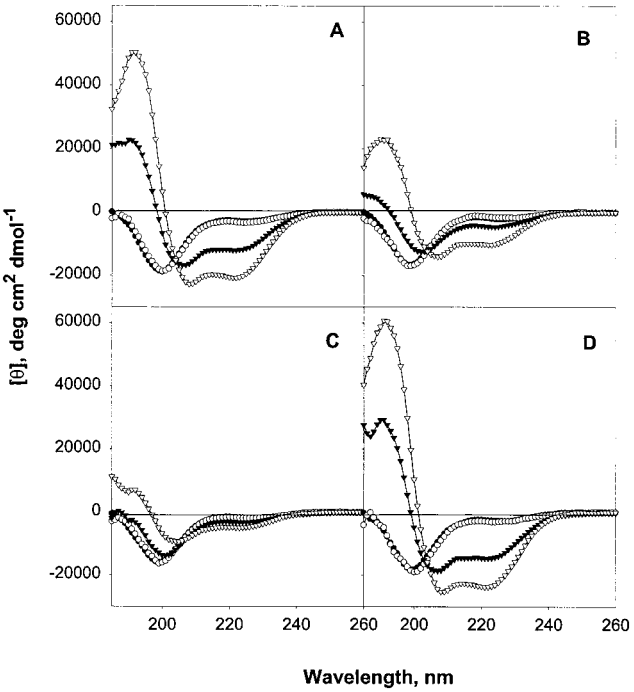

FIGURE 4: Circular dichroic spectra of SCP_2 N-terminal peptides in the presence of SUV with different anionic phospholipid (DOPS) contents. Circular dichroic spectra were obtained as described in Experimental Procedures. Panels: A, peptide $^{1-32}SCP_2$; B, $^{1-24}SCP_2$; C, peptide $^{1-E20-32}SCP_2$; D, peptide $^{10-32}SCP_2$. Symbols refer to the peptides CD spectra taken in the presence of (●) buffer only; (○) SUV, POPC:cholesterol:DOPS = 65:35:0; (▼) SUV, POPC:cholesterol:DOPS = 55:35:10; and (▽) SUV, POPC:cholesterol:DOPS = 35:35:30.

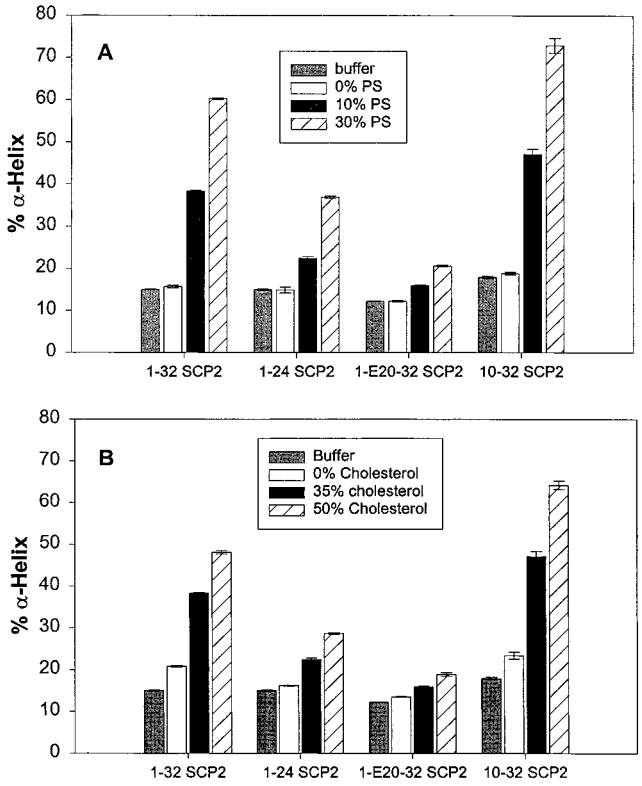

FIGURE 5: Effect of SUV lipid composition on α-helical content of SCP_2 N-terminal peptides upon membrane interaction. Panels: A, α-helical content of SCP_2 N-terminal peptides in the presence of buffer alone and in the presence of SUV with increasing amounts of DOPS (POPC:cholesterol:DOPS = 65:35:0, 55:35:10, 35:35:30); B, α-helical content of SCP_2 N-terminal peptides in the presence of buffer only and in the presence of SUV with increasing amounts of cholesterol (POPC:cholesterol:DOPS = 90:0:10, 55:35:10, 40:50:10). The data are presented as the mean ± SD (n = 4).

chroic spectra of the peptide were increasingly altered with increasing anionic phospholipid in the SUV [Figure 4A, solid triangles (POPC:cholesterol:DOPS mole ratio of 55:35:10) and open triangles (POPC:cholesterol:DOPS mole ratio of 35:35:30) vs solid circles (POPC:cholesterol mole ratio of 65:35)]. In the presence of the negatively charged SUV, the circular dichroic spectra of peptide $^{1-32}SCP_2$ showed typical α- helix characteristics: double negative peaks at 222 and 208 nm and a large positive peak at 190 nm. The isodichroic point at about 205 nm suggested the structure transformation was from random coil to α-helix. Calculations based on molar ellipticity at 222 nm yielded 38% and 60% α-helix for peptide $^{1-32}SCP_2$ in the presence of SUV containing 10% DOPS and 30% DOPS, respectively (Figure 5A). The results indicate that peptide $^{1-32}SCP_2$ preferentially interacted with negative charged vesicles and adopted an α-helical conformation upon interaction. The interaction was stronger with increasing mole percent of anionic lipid PS.

Circular dichroism spectra for peptide $^{1-24}SCP_2$ upon interaction with negatively charged SUV (Figure 4B) were qualitatively similar to those for $^{1-32}SCP_2$ (Figure 4A), except that the changes were significantly smaller. Like $^{1-32}SCP_2$, $^{1-24}SCP_2$ did not undergo secondary structural alterations with neutral SUV but became more α-helical upon interaction with negative SUV. In addition, the α-helical content of peptide $^{1-24}SCP_2$ increased with increasing PS content in the SUV. However, this peptide's interaction with negative SUV was weaker than for $^{1-32}SCP_2$, the amount of α-helix formed in the presence of negative SUV (30% DOPS) reaching only 37% (Figure 5A). This was only 55% of the maximum α-helix formed by peptide $^{1-24}SCP_2$ in TFE/water (1:1) (Table 2). In summary, deletion of the second N-terminal α-helix significantly weakened (about one-third less) the ability of the peptide to interact with negatively charged SUV membranes. However, the second N-terminal α-helix was not essential for the interaction with membranes.

In contrast to the above peptides, both of which interacted with negatively charged SUV, circular dichroic spectral changes for peptide $^{1-E20-32}SCP_2$ showed only small changes in the presence of negative SUV (Figure 4C). Like $^{1-32}SCP_2$, $^{1-E20-32}SCP_2$ did not undergo secondary structural changes with neutral SUV but became more helical upon interaction with negative SUV. Its α-helical content increased with increasing DOPS content in the SUV (Figure 5A). However, this peptide's interaction with negative SUV was much weaker than $^{1-32}SCP_2$. The amount of α-helix formed in the presence of negatively charged SUV (30% DOPS) reached only 21% (Figure 5A). This was only 50% of the maximum α-helix formed by peptide $^{1-E20-32}SCP_2$ in TFE/water (1:1) (Table 2).

Circular dichroic spectral changes for peptide $^{10-32}SCP_2$ upon interaction with negative SUV (Figure 4D) were very similar to those for peptide $^{1-32}SCP_2$ (Figure 4A). Like $^{1-32}SCP_2$, $^{10-32}SCP_2$ did not undergo secondary structural alterations in the presence of neutral SUV but became more α-helical upon interaction with negative SUV (Figures 4D and 5A). The α-helical content of peptide $^{10-32}SCP_2$ increased with increasing PS content in the SUV. The amount of

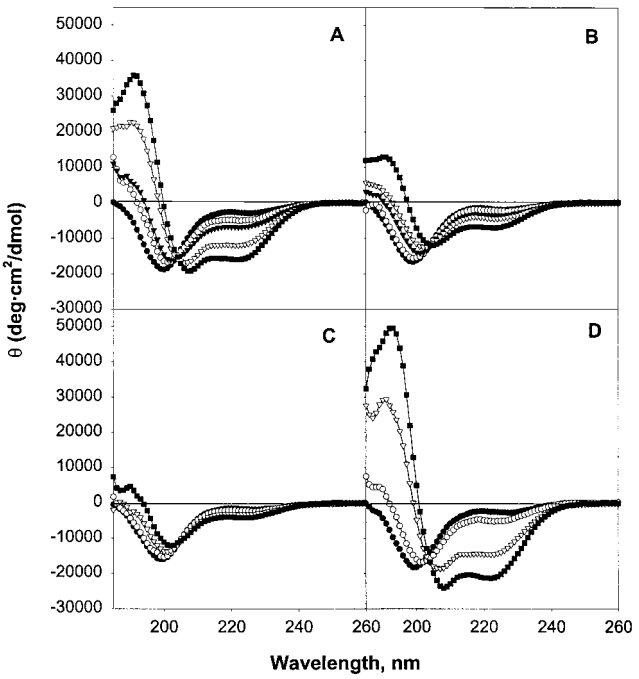

FIGURE 6: Circular dichroic spectra of SCP_2 N-terminal peptides in the presence of SUV with different cholesterol contents. Circular dichroic spectra were obtained as described in Experimental Procedures. Panels: A peptide $^{1-32}SCP_2$; B, $^{1-24}SCP_2$; panel C, peptide $^{1-E20-32}SCP_2$; panel D, peptide $^{10-32}SCP_2$. Symbols refer to the peptide CD spectra taken in the presence of (●) buffer only; (○) SUV, POPC:cholesterol:DOPS = 90:0:10; (▼) SUV, POPC:cholesterol:DOPS = 70:20:10, (▽) SUV, POPC:cholesterol:DOPS = 55:35:10; and (■) SUV, POPC:cholesterol:DOPS = 40:50:10.

α-helix formed in the presence of negatively charged SUV (30% PS) reached 73% (Figure 5A). This was 85% of the maximum α-helix formed by peptide $^{10-32}SCP_2$ in TFE/water (1:1) (Table 2). Thus, deletion of the first nine nonhelical amino acids had no effect on the α-helical formation of the rest of the peptide and had no effect on the membrane interaction of the rest of the peptide.

In summary, all of the four SCP_2 N-terminal peptides preferentially interacted with negatively charged SUV membranes and adopted a more α-helical conformation upon interaction. The interactions were stronger with increasing amounts of negatively charged phospholipid (DOPS) present in the SUV membranes. While deletion of the first nine nonhelical amino acids had no effect on membrane interaction of the rest of the peptide, membrane interactions of peptide $^{1-24}SCP_2$ and even more so peptide $^{1-E20-32}SCP_2$ were significantly weaker than those of peptide $^{1-32}SCP_2$.

Effect of SUV Cholesterol Content on Membrane Interaction of SCP_2 N-Terminal Peptides. The above studies showed that the SCP_2 peptides interacted most strongly with POPC/cholesterol SUV containing anionic phospholipid. Next, we examined the effect of cholesterol content on peptide membrane interaction. Although the anionic phospholipid content of most membranes is maintained in a fairly narrow range, the cholesterol content of intracellular membranes varies widely. Cholesterol content ranges from >50 mol % in cholesterol-rich membranes (e.g., plasma membranes) to 4−10 mol % in cholesterol-poor membranes (e.g., retinal rod outer segment and inner mitochondrial membranes) (reviewed in refs *2*, *4*, *63*, and *64*). Furthermore, microdomains such as plasma membrane caveolae have 3−4-fold as much cholesterol as the surrounding plasma membrane (reviewed in ref *65*).

The effect of increasing cholesterol content from 0 to 50 mol % on circular dichroism spectra of peptide $^{1-32}SCP_2$ interacting with negatively charged SUV membranes (DOPS, 10 mol %) is shown in Figure 6A. In the absence of cholesterol, i.e., POPC:DOPS at a molar ratio of 90:10, the anionic SUV interacted much less strongly with the peptides. With increasing amounts of cholesterol in the anionic SUV, the peptide became substantially more α-helical upon membrane interaction as indicated by the molar ellipticity at 222 nm becoming more negative and molar ellipticity at 190 nm becoming more positive. The isodichroic point at 205 nm suggested that the peptide structure changed from random coil to α-helix. At the highest content of membrane cholesterol content tested (50 mol %) in the anionic SUV, the percent α-helix of peptide $^{1-32}SCP_2$ increased 3.2-fold as compared to peptide $^{1-32}SCP_2$ in aqueous buffer and 2.3-fold as compared to peptide $^{1-32}SCP_2$ interacting with anionic SUV with 0% cholesterol (Figure 5B). As indicated in the preceding section, the presence of cholesterol alone was insufficient for peptide interaction with the neutral SUV, i.e., no circular dichroic spectral changes upon interaction with neutral SUV-containing POPC:cholesterol (65:35). Thus, both cholesterol and anionic phospholipid were necessary for optimal interaction with N-terminal peptides.

Panels B and C of Figure 6 show the circular dichroic spectra of peptides $^{1-24}SCP_2$ and $^{1-E20-32}SCP_2$ in buffer and in the presence of SUV (10% DOPS) with cholesterol content ranging from 0 to 50 mol %. As described above for peptide $^{1-32}SCP_2$, in the absence of cholesterol (POPC:DOPS molar ratio 90:10), the anionic SUV interacted much less strongly with either peptide. With increasing amounts of cholesterol in anionic SUV, the peptide became more α-helical upon membrane interaction. The molar ellipticity at 222 nm became more negative and the molar ellipticity at 190 nm became more positive (Figure 6B,C). The isodichroic point at 205 nm in both panels suggests that the structure of both peptides changed from random coil to more α-helix. However, compared with peptide $^{1-32}SCP_2$, peptides $^{1-24}SCP_2$ and $^{1-E20-32}SCP_2$ interacted much less strongly with the membrane even at the highest cholesterol content (50 mol %).

The amount of α-helix formed by peptides $^{1-24}SCP_2$ and $^{1-E20-32}SCP_2$ in the presence of negative SUV (50% cholesterol) reached only 29% and 19% (Figure 5B). This was only 43% (for peptide $^{1-24}SCP_2$) and 46% (for $^{1-E20-32}SCP_2$) of the maximum α-helix formed by these peptides in TFE/water (1:1). In contrast, peptide $^{1-32}SCP_2$ reached 64% of the maximum α-helix formed by $^{1-32}SCP_2$ in TFE/water (1:1) (Table 2).

The effect of increasing cholesterol content in anionic SUV (10% PS) on circular dichroic spectra of peptide $^{10-32}SCP_2$ (Figure 6D) mimicked that of peptide $^{1-32}SCP_2$ (Figure 6A). As for peptide $^{1-32}SCP_2$, in the absence of cholesterol (POPC:DOPS molar ratio 90:10) the anionic SUV interacted much less strongly with the peptide. With increasing amounts of cholesterol in anionic SUV, peptide $^{10-32}SCP_2$ became more α-helical (64% α-helix at 50 mol % cholesterol). These results indicated that deletion of the first nine nonhelical amino acids had no effect on the α-helical formation of the rest of the peptide in cholesterol-rich anionic SUV.

Table 3: Effect of Cholesterol Content on SUV PS Distribution[a]

composition of SUV, POPC:chol:DOPS	amount of PS (μmol)[b] outer leaflet	total	PS distribution outer leaflet/total
90:0:10	0.41 ± 0.04	0.66 ± 0.07	0.62
70:20:10	0.49 ± 0.03	0.78 ± 0.05	0.63
55:35:10	0.49 ± 0.03	0.83 ± 0.08	0.59
40:50:10	0.35 ± 0.03	0.63 ± 0.09	0.56

[a] PS distribution was measured by TNBS assay as described in Experimental Procedures. [b] Results are presented as mean ± SD (n=3).

In summary, all four SCP_2 N-terminal peptides preferentially interacted with negatively charged SUV membranes containing a high mole percent of cholesterol and adopted a more α-helical conformation upon interaction. The presence of cholesterol alone was insufficient to induce interaction of the peptides with SUV. Both cholesterol and anionic phospholipid were necessary for optimal interaction with N-terminal peptides. The interactions were stronger with increasing amounts of cholesterol present in the negative SUVs. While deletion of the first nine nonhelical amino acids had no effect on membrane interaction of the rest of the peptide, peptide $^{1-24}SCP_2$ and $^{1-E20-32}SCP_2$ interactions with membranes were weaker than those of $^{1-32}SCP_2$.

Effect of SUV Cholesterol Content on Transbilayer Distribution of Anionic Phospholipid. Because increasing the phosphatidylserine content of the SUV increased the ability of the SCP_2 N-terminal peptides to interact with the membranes (see Figures 4 and 5), perhaps increasing the mole percent of cholesterol increased the exposure of phosphatidylserine on the surface of the SUV membranes. To test this possibility, the transbilayer distribution of DOPS was tested in SUV containing 10 mol % DOPS and increasing mole percent cholesterol (Table 3). On the basis of total lipid and the radius of curvature of SUV it was determined that total lipid was distributed across the SUV bilayer such that 70% and 30% of the total lipid were in the outer and inner leaflets, respectively (*58*, *66*). As shown in Table 3, the transbilayer distribution of DOPS in SUV (67% and 33% in the outer and inner leaflets) was nearly the same as that for total lipid transbilayer distribution. Furthermore, increasing the mole percent of cholesterol from 0 to 50 mol % did not significantly increase the quantity of DOPS appearing in the outer leaflet of the SUV membrane (Table 3). If anything, the ratio of outer leaflet/total phosphatidylserine tended to decrease slightly. However, this trend was not statistically significant.

Direct Binding of SCP_2 to SUV. The preceding sections demonstrated extensive circular dichroic changes in SCP_2 upon interaction with SUV rich in acidic phospholipid and cholesterol (e.g., POPC:cholesterol:DOPS = 35:35:30). To confirm that these changes were due to binding to the SUV, an independent direct binding assay was developed. SCP_2 was incubated with SUV (POPC:cholesterol:DOPS = 35:35:30) at room temperature for 10 min, free and unbound SCP_2 were separated by filtration through a 100 kDa molecular cutoff filter, and free (unbound) and membrane-bound SCP_2 were quantitated by SDS−PAGE and gel documentation image analysis as described in Experimental Procedures. The SCP_2 in the assay was maintained constant at 1.55 nmol while SUV (POPC:cholesterol:DOPS = 35:35:30) was varied over the range 0−200 nmol. Representative gel images are given in Figure 7. An SCP_2 standard curve is shown in lanes 1−6 loaded with increasing SCP_2 in amounts of 0, 0.31, 0.62, 0.93, 1.24, and 1.55 μg, respectively. Lanes 7−12 were loaded with fractions containing free (unbound) SCP_2 (Figure 7A) and membrane-bound SCP_2 (Figure 7B) after SCP_2 was incubated with SUV at lipid/protein ratios of 0, 13, 40, 65, 100, and 130, respectively. In the absence of SUV (lane 7), all of the SCP_2 was recovered in the flow-through fraction (designated free or unbound). With increasing amounts of SUV, the amount of free SCP_2 decreased, while the amount of membrane-bound SCP_2 increased. At lipid/protein ratios above 100 (lanes 11 and 12), all of the SCP_2 was recovered in the membrane-bound fraction (Figure 7B) and no free SCP_2 (Figure 7A) was detected. Quantitative analysis of these and other gel images showed that, in the range of lipid/protein ratio 0−60, the increase in percent bound SCP_2 and decrease in percent free SCP_2 were almost linear (Figure 8). At SUV lipid/protein ratios >60, basically there were only small changes in both fractions. In the circular dichroism studies described in the preceding sections, a SUV lipid to SCP_2 protein ratio of 250 was used to ensure maximum binding.

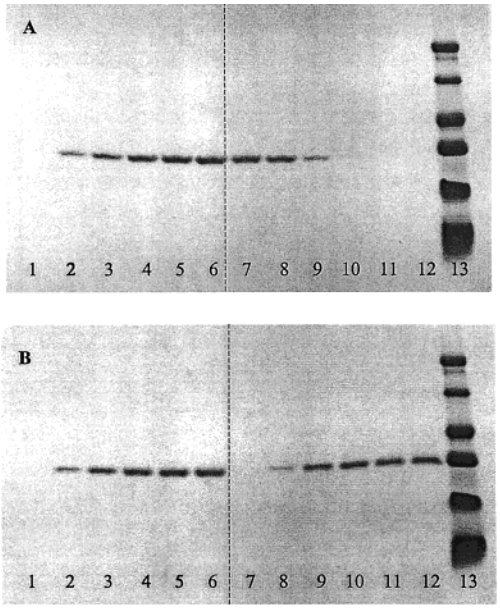

FIGURE 7: Representative gel images of SCP_2 binding to SUV. SCP_2 were incubated with SUV (POPC:cholesterol:DOPS = 35:35:30) at lipid/protein ratios of 0, 13, 40, 65, 100, and 130, respectively, and free and membrane-bound SCP_2 were resolved and quantitated by SDS−PAGE as described in Experimental Procedures. Lanes 1−6 were loaded with SCP_2 standards (0, 0.31, 0.62, 0.93, 1.24, and 1.55 μg, respectively). Lanes 7−12 were loaded with samples from flow through fractions containing free SCP_2 (panel A) and membrane-bound SCP_2 fractions (panel B).

Direct Binding of Peptide to SUV. As mentioned above, in the presence of neutral charged SUV membranes, circular dichroic spectra and α-helical contents of all four SCP_2 N-terminal peptides exhibited very little change as compared with peptides in buffer alone. Also, upon interaction with negatively charged SUV membranes, peptide $^{1-24}SCP_2$ and even more so peptide $^{1-E20-32}SCP_2$ underwent smaller changes in circular dichroic spectra and α-helical content as compared to peptide $^{1-32}SCP_2$. These observed smaller changes could be due to two reasons: first, fewer peptides bound to the SUV membranes; second, upon binding,

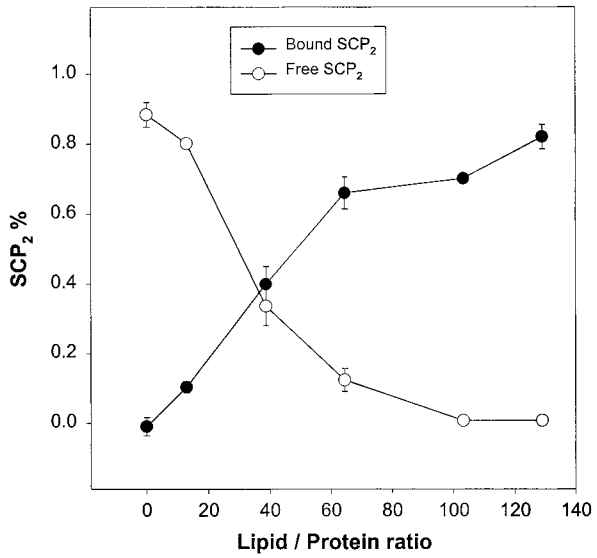

FIGURE 8: Quantitative analysis of SUV-bound and free SCP_2. All procedures were as described in Figure 7. Symbols (●) free SCP_2; (○) SUV membrane-bound SCP_2. Values represent the mean ± SD ($n = 3-4$)

Table 4: SCP_2 N-Terminal Peptide Binding to SUV[a]

SCP_2 N-terminal peptides	free peptide (%)[b]	
	SUV, 65:35:0[c]	SUV, 35:35:30[c]
$^{1-32}SCP_2$	100.0 ± 2.1	26.6 ± 1.2
$^{1-24}SCP_2$	96.7 ± 2.8	53.2 ± 1.4
$^{1-E20-32}SCP_2$	96.0 ± 2.9	77.9 ± 2.4
$^{10-32}SCP_2$	101.2 ± 3.4	29.6 ± 1.4

[a] SCP_2 binding to SUV was done as described in Experimental Procedures. [b] SUV lipid composition refers to POPC:chol:DOPS. [c] Values represent the mean ± SD (n=4).

peptides underwent less secondary structural changes. To resolve these possibilities, the extent of peptide binding to SUV was determined by an independent direct binding assay. The peptides were incubated with SUV (peptide/lipid ratio kept the same as in circular dichroism experiments), and the unbound peptide was separated from the bound peptide by filtration through a 100 000 molecular weight cutoff filter. The free peptides in the flow-through portion were then quantified with an *o*-phthaldialdehyde assay. Table 4 shows the result of the binding assay.

After incubation with neutral charged SUV membranes (POPC:cholesterol = 65:35), 100% of $^{1-32}SCP_2$, 97% of $^{1-24}SCP_2$, 96% of $^{1-E20-32}SCP_2$, and 100% of $^{10-32}SCP_2$ were unbound (Table 4). Therefore, none of the peptides showed significant binding to neutral charged membranes. This indicated that the observed lack of changes in circular dichroic spectra of the peptides in the presence of neutral membrane vesicles was due to lack of binding of the peptides to neutral charged SUV membranes.

In the presence of negatively charged SUV membranes (POPC:cholesterol:DOPS = 35:35:30), the percentage of unbound peptides significantly decreased to 27% for $^{1-32}SCP_2$, 53% for $^{1-24}SCP_2$, 78% for $^{1-E20-32}SCP_2$, and 30% for $^{10-32}SCP_2$ (Table 4). The results indicate that all peptides preferentially bound to negatively charged SUV membranes in the following order: $^{1-32}SCP_2$, $^{10-32}SCP_2$ > $^{1-24}SCP_2$ > $^{1-E20-32}SCP_2$. The data obtained with the binding assay were consistent with those obtained by circular dichroism and

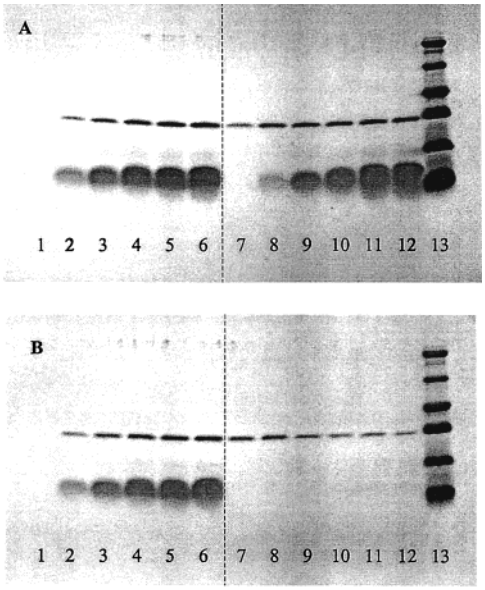

FIGURE 9: Representative gel images of displacement of SUV-bound SCP_2 by the N-terminal peptide $^{1-32}SCP_2$. SCP_2 was bound to SUV (POPC:cholesterol:DOPS = 35:35:30) at a lipid/SCP_2 protein ratio of 40, followed by addition of the N-terminal peptide $^{1-32}SCP_2$. Lanes 1−6 were loaded with standard solutions of SCP_2 in amounts of 0, 0.31, 0.62, 0.93, 1.24, and 1.55 μg, respectively. Lanes 7−12 were loaded with fractions of free (panel A) and membrane-bound SCP_2 (panel B) after SCP_2 was incubated with SUV and N-terminal peptide $^{1-32}SCP_2$ at peptide/protein ratios of 0, 2.5, 7.5, 12.5, 20, and 25, respectively.

indicated that (1) substitution of Leu^{20} with Glu^{20} decreased the membrane binding ability of this peptide to negatively charged SUV membranes by 3.3-fold, (2) deletion of the second predicted α-helix had a much smaller effect by decreasing binding of the peptide to negatively charged SUV membranes by 36%, and (3) deletion of the first nine nonhelical amino acids had no effect on peptide binding to negatively charged SUV membranes.

Displacement of SUV-Bound SCP_2 by Peptide. The circular dichroism and the direct binding assays described above indicated that the SCP_2 N-terminal is a membrane-binding domain. Like SCP_2, the N-terminal peptide $^{1-32}SCP_2$ preferentially bound to lipid membranes rich in negatively charged lipid and rich in cholesterol. The following experiments were performed to determine if the N-terminal peptide competed with SCP_2 on binding to membrane vesicles. In these experiments, SCP_2 and SUV were incubated in the presence and absence of the N-terminal peptide $^{1-32}SCP_2$, and displacement of bound SCP_2 by peptide was determined as described in Experimental Procedures.

A displacement experiment was carried out to study the effect of the SCP_2 N-terminal peptide on SCP_2 binding to lipid membrane vesicles. In this experiment, a lipid/protein ratio of 40, close to the middle of the linear range on the SCP_2 binding curve (Figure 8), was used in order to easily determine either increased or decreased binding. A representative gel image of the displacement experiment is given in Figure 9. Lanes 1−6 were loaded with standard solutions of SCP_2 in amounts of 0, 0.31, 0.62, 0.93, 1.24, and 1.55 μg, respectively. When known amounts of peptide $^{1-32}SCP_2$ were also loaded together with standard SCP_2 in these lanes in order to simultaneously quantitate the peptide, at high peptide concentrations the peptide signals are saturated and

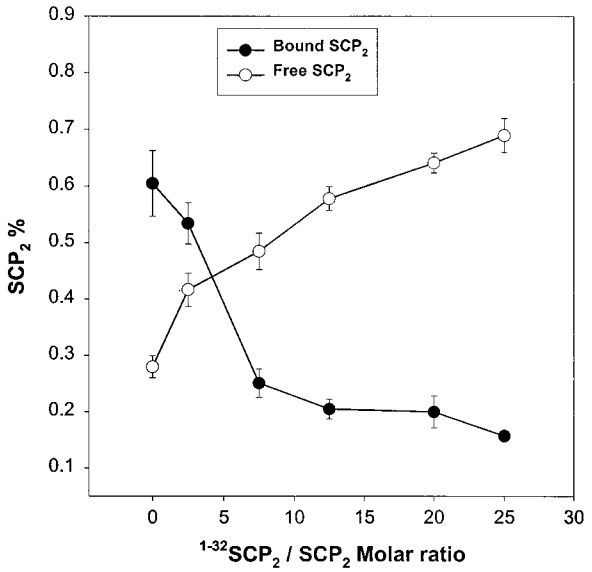

FIGURE 10: Quantitative analysis of displacement of SUV-bound SCP_2 by the N-terminal peptide $^{1-32}SCP_2$. All procedures were as described in Figure 9. (●) free SCP_2; (○) SUV membrane-bound SCP_2. Values represent the mean ± SD ($n = 3-4$).

a good quantitation was difficult to obtain. Therefore, only the free (Figure 9A, lanes 7−12) and bound (Figure 9B, lanes 7−12) SCP_2 proteins were quantitated after SCP_2 and SUV were incubated with increasing ratios (0, 2.5, 7.5, 12.5, 20, and 25) of N-terminal peptide $^{1-32}SCP_2$ to SCP_2 protein in lanes 7−12, respectively. As shown in the gel, with increasing peptide/protein ratio the amount of free SCP_2 decreased while the amount of bound SCP_2 increased. Quantitative analysis of these and additional gel images is shown in Figure 10. At a lipid/protein ratio of 40 and in the absence of the SCP_2 N-terminal peptide $^{1-32}SCP_2$, 60% of the SCP_2 added was recovered as free protein while the remaining 28% of SCP_2 added was recovered in the SUV membrane-bound fraction. With increasing amounts of N-terminal peptide $^{1-32}SCP_2$ added, the amount of free SCP_2 increased and while the amount of membrane-bound SCP_2 decreased. At a ratio of peptide $^{1-32}SCP_2/SCP_2$ protein of 25, only 16% of the SCP_2 added was bound, and about 70% of SCP_2 added was free. Thus, N-terminal peptide $^{1-32}SCP_2$ competed with SCP_2 for binding to SUV membranes.

DISCUSSION

Although the function of SCP_2 has been investigated for more than two decades, very little is known regarding either the tertiary or secondary structure of apo-SCP_2. Both NMR and intrinsic fluorescence data show that the 13 kDa SCP_2 is a slightly ellipsoid globular protein (*11*, *61*, *67*). SCP_2 appears to be comprised of at least two structurally important domains:

First, SCP_2 has a ligand binding domain/site. Until recently, the existence and nature of an SCP_2 ligand binding site were unresolved. Many different techniques including functional assays, radioligand binding, light scattering, fluorescent sterol binding, and NMR have been used to establish that SCP_2 binds cholesterol with 1:1 stoichiometry and affinity measured as low as 6 nM (*2*, *36*−*39*).[3] Furthermore, recent exciting data pointing out new potential functions of SCP_2 indicate that SCP_2 also interacts with high affinity with fatty acids, fatty acyl-CoAs, and isoprenoids (*9*−*12*, *15*). The observation that SCP_2 binds isoprenyl pyrophosphates with high affinity (*12*) may account for the ability of SCP_2 to dramatically enhance isoprenyltransferase activity to form dolichol (*13*). Finally, fluorescence studies show that the binding of ligand is essential for SCP_2's ability to transfer the ligand between membranes (*68*). However, the amino acids comprising the ligand binding site(s) of SCP_2 have not yet been defined.

Second, the SCP_2 N-terminal contains two amphipathic α-helical regions hypothesized to represent the SCP_2 domain interacting with membranes (*50*, *61*). Circular dichroic investigations of mutant apo-SCP_2's in aqueous buffer suggest that disruptions and/or deletions of portions of the N-terminus dramatically reduce the α-helical content of the protein and abolish its lipid transfer activity (*44*). However, since ligand binding studies were not reported with these mutant proteins, it is unclear whether the ligand binding site, the membrane interaction site, or both were disrupted in the mutagenized SCP_2. Several early reports based on primary sequence and structure analysis (*50*) as well as effects on SCP_2 on sterol transfer between model membranes (*32*, *45*−*49*, *69*) provided indirect data leading to the hypothesis that the SCP_2 amino terminus may form a membrane interaction site. However, the nature of this putative SCP_2 membrane-binding domain is unresolved. The purpose of the present investigation was to obtain direct evidence addressing whether SCP_2 or its N-terminal peptides interact with lipid membranes, determine if SCP_2 and its N-terminal peptides change their secondary structures upon membrane interaction, examine some of the structural requirements in the SCP_2 N-terminus that are required for membrane interaction, and define the effect of membrane lipid composition on the SCP_2 and N-terminal peptide membrane interaction.

The data presented herein utilized both a direct binding assay and circular dichroism to demonstrate for the first time that SCP_2 binds to membranes. A direct filtration assay showed that SCP_2 protein bound to SUV membranes rich in anionic phospholipid and cholesterol. Furthermore, circular dichroism showed that SCP_2 underwent secondary structural changes upon interaction with anionic, cholesterol-rich lipid vesicles. Upon membrane interaction, SCP_2 underwent secondary structural changes favoring nearly an 8% increase in α-helix formation. This finding was distinct from that observed for interaction of SCP_2 with ligand cholesterol alone in the absence of membranes, where a 3% decrease in SCP_2 α-helix was reported (*37*). These opposing effects of ligand binding and membrane binding allow postulation of the following speculation regarding a potential "hopping" mechanism whereby SCP_2 may mediate intermembrane sterol exchange: In such a hopping mechanism, the SCP_2 would bind to anionic phospholipid-containing, cholesterol-rich membrane to undergo conformational changes resulting in increased α-helix content. Such a conformational change would increase exposure of the SCP_2 cholesterol binding site to the membrane-bound cholesterol—i.e., optimize/favor interaction with membrane-bound ligand. Upon cholesterol binding to the SCP_2 ligand binding site, the SCP_2 would undergo the opposite conformational change to decrease α-helix content and decrease membrane binding without decreasing ligand binding. This would elicit removal of cholesterol from the bilayer. A similar hopping mechanism

was first suggested for phospholipase A2 (*70*). There have been few earlier studies directly addressing the binding of SCP_2 to membranes and, to our knowledge, no previous reports on the effect of membrane interaction on the secondary structure of SCP_2. Our laboratory earlier reported that SCP_2 interaction with biological membranes slowed the rotation rate of the protein (*41*). Likewise, another study of SCP_2 interaction with anionic monolayers showed that SCP_2 increased the surface pressure of the monolayer (*69*).

Identification of a putative membrane-binding domain of SCP_2 has not previously been established. NMR structure analysis of the complete SCP_2 protein showed that the N-terminal region was comprised of two α-helical regions, peptide residues 9−22 and 25−30, and an additional small α-helix at residues 78−84 (*61*). Because acidic phospholipids, such as phosphatidylinositol, phosphatidylserine, or cardiolipin, in membranes markedly enhance SCP_2-mediated sterol transfer while high ionic strength and neomycin abrogate this effect, electrostatic interactions are important for the activity of SCP_2 (*47*). Consequently, it was postulated that the lysines in the N-terminal amphipathic α-helix (Figure 2) may interact with the negatively charged residues of the acidic phospholipid in the sonicated SUV membrane bilayer (*47*, *71*). The circular dichroism and binding data presented herein with peptide $^{1-32}SCP_2$ (containing the complete SCP_2 N-terminal α-helical region) showed for the first time that this region of SCP_2 comprised a membrane-binding domain that interacted most favorably with membranes rich in anionic phospholipid and cholesterol. These findings were consistent with those observed with the intact SCP_2 protein. Finally, a displacement experiment clearly demonstrated that N-terminal peptide $^{1-32}SCP_2$ inhibited the binding of SCP_2 to anionic, cholesterol-rich lipid vesicles.

To determine which structural requirements within the SCP_2 N-terminus were essential for providing a membrane interaction site in the absence of other parts of the SCP_2 molecule, several N-terminal peptides were synthesized and their ability to interact with membranes was examined. The peptides studied were $^{1-32}SCP_2$ (contained the complete SCP_2 N-terminal α-helical region), $^{1-24}SCP_2$ (deletion of the second α-helical region), $^{1-E20-32}SCP_2$ (substitution of Leu^{20} with Glu^{20}), and $^{10-32}SCP_2$ (deletion of the first nine nonhelical amino acids). The binding of the peptides to lipid vesicles was monitored by circular dichroism measurement. The secondary structure changes upon membrane interaction were determined on the basis of circular dichroism data. The amount of secondary structure changes of the peptides upon membrane interaction depends on their ability to bind to the membranes and their ability to form an α-helix after binding. Therefore, a direct binding assay was performed to determine how much of the peptides actually bound to the membrane, and circular dichroic spectra of the peptides in 50% aqueous TFE solution was measured to determine the ability of the peptides to form an α-helix. The results indicate the following:

(i) Deletion of the second helical region had no effect on the first helix formation. Circular dichroic spectra of peptides $^{1-32}SCP_2$ and $^{1-24}SCP_2$ in aqueous TFE indicated that both peptides had about eight nonhelical amino acids and the rest of the amino acids formed an α-helix. This was consistent with NMR data which predicted that the first nine amino acids of the SCP_2 N-terminal are not helical. However, peptide $^{1-24}SCP_2$ had weaker binding to membranes compared with peptide $^{1-32}SCP_2$, as indicated by both the binding assay and circular dichroic spectral changes in the presence of membranes. This may indicate that the second helical region played an important role for membrane interaction or the interaction is weakened because of the charge repulsion (peptide $^{1-24}SCP_2$ has two net negative charges, while $^{1-32}SCP_2$ has only one).

(ii) Substitution of Leu^{20} with Glu^{20} disrupted the ability of the peptide to form an α-helix. Circular dichroism data of peptides in aqueous TFE indicated that peptide $^{1-E20-32}SCP_2$ had only about 13 helical amino acids while peptide $^{1-32}SCP_2$ had about 24. The substitution also greatly decreased its membrane interaction as indicated by direct binding assay and very little circular dichroic spectral changes upon membrane interaction, compared with peptide $^{1-32}SCP_2$. The weakened membrane interaction could be due to the disrupted α-helix and the charge repulsion between the negative charges (peptide $^{1-E20-32}SCP_2$ has two net negative charges, while $^{1-32}SCP_2$ has only one). Impaired membrane interaction could account for the loss of intermembrane sterol transfer activity in SCP_2 protein mutated by replacing Leu^{20} with Glu^{20} (*44*).

(iii) Deletion of the first nine nonhelical amino acids had no effect on the helical structure formation of the rest of the peptide. Circular dichroism of peptide $^{10-32}SCP_2$ in aqueous TFE indicated that peptide $^{10-32}SCP_2$ had only about three nonhelical amino acids. Deletion of the first nine amino acids also had no effect on peptide interaction with lipid vesicles. This indicated that the loss of intermembrane sterol transfer activity after deletion of the first nine amino acids in the mutant SCP_2 (*44*) was not due to inability to interact with membranes.

The circular dichroic and binding studies indicated that all peptides analyzed had higher affinity for anionic than neutral zwitterionic lipids, consistent with an electrostatic component to the binding. All four SCP_2 N-terminal peptides showed mostly random structure in aqueous buffer. The peptides preferentially interacted with negatively charged lipid vesicles and adopted an α-helical conformation. Helical wheel projections (Figure 3) showed that some basic side chains were positioned along the polar and nonpolar interfaces, while the acidic side chains were mostly segregated to the center of the polar face. This explains why even though all the peptides have a net negative charge (−1 or −2), they all have preference for anionic lipids. The helical wheel projections also provide insight into why the mutant peptide, $^{1-E20-32}SCP_2$, was inactive. Compared to $^{1-32}SCP_2$, peptide $^{1-E20-32}SCP_2$ has a single substitution at position 20. Helical wheel projection shows that position 20 is in the middle of the hydrophobic region of the helix. Substitution of a hydrophobic amino acid Leu^{20} with a negatively charged amino acid such as Glu^{20} would disrupt part of the α-helical structure. Primary amino acid sequence analysis predicted an interrupted α-helical region. Site-directed mutagenesis of SCP_2 revealed that mutations (substitution of Leu^{20} with Glu^{20}) perturbed the nature of the α-helix (altered the circular dichroic spectrum of the mutant SCP_2 protein) and destroyed its ability to stimulate intermembrane sterol transfer (*44*). The physiological relevance of the present findings showing interaction of the N-terminus with anionic phospholipid containing SUV is supported by an earlier study with intact

SCP_2 showing that direct interaction of the protein with biological membranes is also required for cholesterol transfer activity (*41*).

Not only anionic phospholipids but also cholesterol was required for the optimal interaction of the SCP_2 N-terminal peptides with SUV. SCP_2 peptides interacted best with anionic SUV containing the highest amount, 50 mol %, of cholesterol; the α-helix content increased 3.2-fold, as compared to aqueous buffer. While the structural basis for the cholesterol effect is not known, the data showed that it was not through increased exposure of anionic phospholipids in the outer leaflet of the SUV membrane. Instead, it is postulated to be through the formation of cholesterol-rich, lateral domains (reviewed in refs *1*, *3*−*5*, *18*, *32*−*34*, and *72*), which may thereby exclude and concentrate the anionic phospholipids into domains that may interact better with the amphipathic N-terminal peptides or the amphipathic N-terminus of the SCP_2 protein. The physiological relevance of the present findings showing interaction of the N-terminus with cholesterol-rich, anionic phospholipid rich membranes is supported by an earlier study with intact SCP_2 showing that SCP_2 stimulated the transfer of cholesterol much more (up to 27−50-fold) from cholesterol-rich intracellular membranes such as plasma membranes and lysosomal membranes, respectively, than from cholesterol-poor mitochondrial membranes (2−4-fold) (*2*, *42*). The molecular basis for the preferential enhancement of sterol transfer from the plasma membrane may be due, at least in part, to the presence of cholesterol-rich domains within the plasma membrane. For example, the cholesterol content of the plasma membrane cytofacial leaflet is 4−5 times higher than that of the exofacial leaflet (*2*−*4*, *73*, *74*). Furthermore, plasma membranes contain microdomains (<1% of total membrane) such as caveolae that have 3−4-fold higher cholesterol content than the rest of the plasma membrane (*65*). Caveolae represent the sites of rapid HDL-mediated cholesterol efflux from the cell (*65*).

In summary, the circular dichroic results obtained herein with intact SCP_2 protein are consistent with SCP_2 undergoing secondary structural alterations upon interaction with membranes. Furthermore, the N-terminal peptide data support the hypothesis that the $^{1-32}SCP_2$ peptide represents a membrane interaction domain. Finally, the interaction of the N-terminal peptides to form increased α-helix was greatest with membranes rich in both anionic phospholipid and cholesterol. The molecular basis for the effect of anionic phospholipids appears to be through electrostatic interactions with the amphipathic α-helix present in the N-terminus.

REFERENCES

1. Vahouny, G. V., Chanderbhan, R., Kharroubi, A., Noland, B. J., Pastuszyn, A., and Scallen, T. J. (1987) *Adv. Lipid Res. 22*, 83−113.
2. Schroeder, F., Frolov, A., Schoer, J., Gallegos, A., Atshaves, B. P., Stolowich, N. J., Scott, A. I., and Kier, A. B. (1998) in *Intracellular Cholesterol Trafficking* (Freeman, D., and Chang, T. Y., Eds.) pp 213−234, Kluwer Academic Publishers, Boston.
3. Schroeder, F., Jefferson, J. R., Kier, A. B., Knittell, J., Scallen, T. J., Wood, W. G., and Hapala, I. (1991) *Proc. Soc. Exp. Biol. Med. 196*, 235−252.
4. Schroeder, F., Frolov, A. A., Murphy, E. J., Atshaves, B. P., Jefferson, J. R., Pu, L., Wood, W. G., Foxworth, W. B., and Kier, A. B. (1996) *Proc. Soc. Exp. Biol. Med. 213*, 150−177.
5. Moncecchi, D. M., Nemecz, G., Schroeder, F., and Scallen, T. J. (1991) in *Physiology and Biochemistry of Sterols* (Patterson, G. W., and Nes, W. D., Eds.) pp 1−27, American Oil Chemists Society Press, Champaign, IL.
6. Wirtz, K. W. A. (1997) *Biochem. J. 324*, 353−360.
7. Ossendorp, B. C., Snoek, G. T., and Wirtz, K. W. A. (1994) *Curr. Top. Membr. 40*, 217−259.
8. Pfeifer, S. M., Furth, E. E., Ohba, T., Chang, Y. J., Rennert, H., Sakuragi, N., Billheimer, J. T., and Strauss, J. F., III (1993) *J. Steroid Biochem. Mol. Biol. 47*, 167−172.
9. Schroeder, F., Myers-Payne, S. C., Billheimer, J. T., and Wood, W. G. (1995) *Biochemistry 34*, 11919−11927.
10. Stolowich, N. J., Frolov, A., Atshaves, B. P., Murphy, E., Jolly, C. A., Billheimer, J. T., Scott, A. I., and Schroeder, F. (1997) *Biochemistry 36*, 1719−1729.
11. Frolov, A., Cho, T. H., Billheimer, J. T., and Schroeder, F. (1996) *J. Biol. Chem. 271*, 31878−31884.
12. Frolov, A., Miller, K., Billheimer, J. T., Cho, T.-C., and Schroeder, F. (1997) *Lipids 32*, 1201−1209.
13. Ericsson, J., Scallen, T., Chojnacki, T., and Dallner, G. (1991) *J. Biol. Chem. 266*, 10602−10607.
14. Seedorf, U. (1998) in *Intracellular Cholesterol Trafficking* (Chang, T. Y., and Freeman, D. A., Eds.) pp 233−252, Kluwer Academic Publishers, Boston.
15. Seedorf, U., Raabe, M., Ellinghaus, P., Kannenberg, F., Fobker, M., Engel, T., Denis, S., Wouters, F., Wirtz, K. W. A., Wanders, R. J. A., Maeda, N., and Assmann, G. (1998) *Genes Dev. 12*, 1189−1201.
16. Batenburg, J. J., Ossendorp, B. C., Snoek, G. T., Wirtz, K. W., Houweling, M., and Elfring, R. H. (1994) *Biochem. J. 298*, 223−229.
17. McLean, M. P., Billheimer, J. T., Warden, K. J., and Irby, R. B. (1995) *Endocrinology 136*, 3360−3368.
18. Pfeifer, S. M., Furth, E. E., Ohba, T., Chang, Y. J., Rennert, H., Sakuragi, N., Billheimer, J. T., and Strauss, J. F. I. (1993) *J. Steroid Biochem. Mol. Biol. 47*, 167−172.
19. Kawata, S., Imai, Y., Inada, M., Inui, M., Kakimoto, H., Fukuda, K., Maeda, Y., and Tarui, S. (1991) *Clin. Chim. Acta 197*, 201−208.
20. Bun-ya, M., Maebuchi, M., Kamiryo, T., Kurosawa, T., Sato, M., Tohma, M., Jiang, L. L., and Hashimoto, T. (1998) *J. Biochem. 123*, 347−352.
21. Fuchs, M., Lammert, F., Wang, D. Q. H., Paigen, B., Carey, M. C., and Cohen, D. E. (1997) Sterol carrier protein-2 but not phosphatidylcholine−gene expression is enhanced during cholesterol gallstone formation in mice, AASLD Meeting, Abstract A-1267.
22. Puglielli, L., Rigotti, A., Amigo, L., Nunez, L., Greco, A. V., Santos, M. J., and Nervi, F. (1996) *Biochem. J. 317*, 681−687.
23. Fuchs, M., Lammert, F., Wang, D. Q. H., Paigen, B., Carey, M. C., and Cohen, D. E. (1997) *FASEB J. 11*, A1060.
24. Ito, T., Kawata, S., Imai, Y., Kakimoto, H., Trzaskos, J., and Matsuzawa, Y. (1996) *Gastroenterology 110*, 1619−1627.
25. Yamamoto, R., Kallen, C. B., Babalola, G. O., Rennert, H., Billheimer, J. T., and Strauss, J. F. I. (1991) *Proc. Natl. Acad. Sci. U.S.A. 88*, 463−467.
26. Chanderbhan, R., Kharroubi, A., Noland, B. J., Scallen, T. J., and Vahouny, G. V. (1986) *Endocrine Res. 12*, 351−370.
27. Chanderbhan, R. F., Kharoubi, A., Pastuszyn, A., Gallo, L. L., and Scallen, T. (1998) in *Intracellular cholesterol trafficking* (Chang, T. Y., and Freeman, D., Eds.) pp 197−212, Kluwer Academic Publishers, Boston.
28. Moncecchi, D. M., Murphy, E. J., Prows, D. R., and Schroeder, F. (1996) *Biochim. Biophys. Acta 1302*, 110−116.
29. Atshaves, B. P., Petrescu, A., Starodub, O., Roths, J., Kier, A. B., and Schroeder, F. (1999) *J. Lipid Res. 40*, 610−622.
30. Murphy, E. J., and Schroeder, F. (1997) *Biochim. Biophys. Acta 1345*, 283−292.
31. Baum, C. L., Reschly, E. J., Gayen, A. K., Groh, M. E., and Schadick, K. (1997) *J. Biol. Chem. 272*, 6490−6498.
32. Hapala, I., Kavecansky, J., Butko, P., Scallen, T. J., Joiner, C., and Schroeder, F. (1994) *Biochemistry 33*, 7682−7690.

33. Billheimer, J. T., and Reinhart, M. P. (1990) *Sub-Cell. Biochem. 16*, 301−331.
34. Zilversmit, D. B. (1984) *J. Lipid Res. 25*, 1563−1569.
35. Gadella, T. W., Jr., and Wirtz, K. W. (1991) *Biochim. Biophys. Acta 1070*, 237−245.
36. Schroeder, F., Butko, P., Nemecz, G., and Scallen, T. J. (1990) *J. Biol. Chem. 265*, 151−157.
37. Colles, S. M., Woodford, J. K., Moncecchi, D., Myers-Payne, S. C., McLean, L. R., Billheimer, J. T., and Schroeder, F. (1995) *Lipids 30*, 795−804.
38. Chanderbhan, R., Noland, B. J., Scallen, T. J., and Vahouny, G. V. (1982) *J. Biol. Chem. 257*, 8928−8934.
39. Sams, G. H., Hargis, B. M., and Hargis, P. S. (1991) *Comput. Biochem. Phys. 99B*, 213−219.
40. Avdulov, N. A., Chochina, S. V., Igbavboa, U., Warden, C. H., Schroeder, F., and Wood, W. G. (1999) *Biochim. Biophys. Acta 1437*, 37−45.
41. Woodford, J. K., Colles, S. M., Myers-Payne, S., Billheimer, J. T., and Schroeder, F. (1995) *Chem. Phys. Lipids 76*, 73−84.
42. Frolov, A., Woodford, J. K., Murphy, E. J., Billheimer, J. T., and Schroeder, F. (1996) *J. Biol. Chem. 271*, 16075−16083.
43. Frolov, A. A., Woodford, J. K., Murphy, E. J., Billheimer, J. T., and Schroeder, F. (1996) *J. Lipid Res. 37*, 1862−1874.
44. Seedorf, U., Scheek, S., Engel, T., Steif, C., Hinz, H. J., and Assmann, G. (1994) *J. Biol. Chem. 269*, 2613−2618.
45. Hapala, I., Butko, P., and Schroeder, F. (1990) *Chem. Phys. Lipids 56*, 37−47.
46. Butko, P., Hapala, I., Nemecz, G., and Schroeder, F. (1992) *J. Biochem. Biophys. Methods 24*, 15−37.
47. Butko, P., Hapala, I., Scallen, T. J., and Schroeder, F. (1990) *Biochemistry 29*, 4070−4077.
48. Gadella, T. W., and Wirtz, K. W. (1994) *Eur. J. Biochem. 220*, 1019−1028.
49. Billheimer, J. T., and Gaylor, J. L. (1990) *Biochim. Biophys. Acta 1046*, 136−143.
50. Pastuszyn, A., Noland, B. J., Bazan, F., Fletterick, R. J., and Scallen, T. J. (1987) *J. Biol. Chem. 262*, 13219−13227.
51. Matsuura, J. E., George, H. J., Ramachandran, N., Alvarez, J. G., Strauss, J. F. I., and Billheimer, J. T. (1993) *Biochemistry 32*, 567−572.
52. Fontenot, J. D., Ball, J. A., Miller, M. A., David, C. M., and Montelaro, R. C. (1991) *Pept. Res. 4*, 19−25.
53. Schroeder, F., Barenholz, Y., Gratton, E., and Thompson, T. E. (1987) *Biochemistry 26*, 2441−2448.
54. Ames, B. N. (1968) *Methods Enzymol. 8*, 115−118.
55. Chen, Y.-H., Yang, J. T., and Chau, K. H. (1974) *Biochemistry 13*, 3350−3359.
56. Chang, C. T., Wu, C.-S. C., and Yang, J. T. (1978) *Anal. Biochem. 91*, 13−31.
57. Sreerama, N., and Woody, R. (1993) *Anal. Biochem. 209*, 32−44.
58. Litman, B. J. (1973) *Biochemistry 12*, 2545−2554.
59. Johnson, J. E., Rao, N. M., Hui, S. W., and Cornell, R. B. (1998) *Biochemistry 37*, 9509−9519.
60. Johnson, J. E., and Cornell, R. B. (1994) *Biochemistry 33*, 4327−4335.
61. Szyperski, T., Scheek, S., Johansson, J., Assmann, G., Seedorf, U., and Wuthrich, K. (1993) *FEBS Lett. 335*, 18−26.
62. Sonnichsen, F. D., Van Eyk, J. E., Hodges, R. S., and Sykes, B. D. (1992) *Biochemistry 31*, 8790−8798.
63. Liscum, L., and Dahl, N. K. (1992) *J. Lipid Res. 33*, 1239−1254.
64. Rose, T. M., Schultz, E. R., Sasaki, G. C., Kolattukudy, P. E., and Shoyab, M. (1994) *DNA Cell Biol. 13*, 669−678.
65. Smart, E. J., and van der Westhuyzen, D. R. (1998) in *Intracellular cholesterol trafficking* (Chang, T. Y., and Freeman, D. A., Eds) pp 253−272, Kluwer Scientific Publishers, Boston.
66. Berden, J. A., Barker, R. W., and Radda, G. K. (1975) *Biochim. Biophys. Acta 375*, 186−208.
67. Gadella, T. W. J., Bastiaens, P. I. H., Visser, A. J. W. G., and Wirtz, K. W. A. (1991) *Biochemistry 30*, 5555−5564.
68. Woodford, J. K., Hapala, I., Jefferson, J. R., Knittel, J. J., Kavecansky, J., Powell, D., Scallen, T. J., and Schroeder, F. (1994) *Biochim. Biophys. Acta 1189*, 52−60.
69. Van Amerongen, A., Demel, R. A., Westerman, J., and Wirtz, K. W. A. (1989) *Biochim. Biophys. Acta 1004*, 36−46.
70. Jain, M. K., Rogers, J., and DeHaas, G. H. (1988) *Biochim. Biophys. Acta 940*, 51−62.
71. Ostenson, C. G., Ahren, B., Karlsson, S., Sandberg, E., and Efendic, S. (1990) *Regul. Pept. 29*, 143−151.
72. Bretscher, M. S., and Munro, S. (1993) *Science 261*, 1280−1281.
73. Schroeder, F., and Nemecz, G. (1990) in *Advances in Cholesterol Research* (Esfahani, M., and Swaney, J., Eds.) pp 47−87, Telford Press, Caldwell, NJ.
74. Schroeder, F., Woodford, J. K., Kavecansky, J., Wood, W. G., and Joiner, C. (1995) *Mol. Membr. Biol. 12*, 113−119.

BI990870X